



Earthquake ground motion prediction using the ambient seismic field

Germán A. Prieto¹ and Gregory C. Beroza¹

Received 23 April 2008; revised 17 June 2008; accepted 20 June 2008; published 22 July 2008.

[1] The waves generated by faulting represent the primary threat posed by most large earthquakes. The effect of complex geological structures, such as sedimentary basins, on earthquake ground motion is a source of particular concern. We show that it is possible to extract reliable phase and amplitude response that includes the effects of complex structure for the elastodynamic Green's function from the ambient seismic field using deconvolution. We demonstrate the accuracy of the approach by predicting complex ground motion for a moderate ($M_w = 4.6$) earthquake in southern California as recorded in the Los Angeles Basin. This suggests a novel approach to seismic hazard analysis in which ground motion from hypothetical future earthquakes is simulated directly, without the need for modeling the detailed heterogeneity of the Earth's crust as an intermediate step.

Citation: Prieto, G. A., and G. C. Beroza (2008), Earthquake ground motion prediction using the ambient seismic field, *Geophys. Res. Lett.*, 35, L14304, doi:10.1029/2008GL034428.

1. Introduction

[2] The strength of ground shaking in hypothetical future earthquakes is typically predicted using ground motion attenuation laws [e.g., *Abrahamson and Shedlock*, 1997]. Attenuation laws are predictions of a specified ground motion intensity measure, such as the peak ground acceleration, based on observations of past earthquakes with known characteristics. These laws codify the dependence of shaking on quantities such as the magnitude of the earthquake and distance from the rupture; however, the strength of shaking is also strongly influenced by the distorting effect of complex geologic structure on the radiated seismic wavefield. The Next Generation Attenuation (NGA) project relations may help somewhat by taking into account basin response effects [*Power et al.*, 2008].

[3] Increasingly, seismologists attempt to predict shaking in future large earthquakes through simulation [*Komatitsch et al.*, 2004; *Olsen et al.*, 2006; *Aagaard et al.*, 2008]. There are a number of sources of uncertainty in such simulations, including: complexities in the earthquake source [*Mai and Beroza*, 2002], unmodeled linear wave propagation effects, such as focusing and basin amplification [*Vidale and Helmberger*, 1988], and ground motion non-linearities, such as soil liquefaction [*Seed and Idriss*, 1971]. Accurate simulation of strong ground motion requires that all these sources of uncertainty be minimized; however, in this study we focus on just one of them: predicting linear wave propagation effects due to complex Earth structure.

[4] A source of particular concern for seismic hazard analysis is the effect of large sedimentary basins on earthquake ground motion. Basin amplification is a major problem for many large urban centers, including metropolitan Los Angeles, because basins trap and amplify seismic energy [*Vidale and Helmberger*, 1988; *Pitarka et al.*, 1998; *Stidham et al.*, 1999; *Komatitsch et al.*, 2004; *Olsen et al.*, 2006], and thereby increase vulnerability to earthquakes. The ability of ground motion simulations to model such effects is critical to reliable seismic hazard analysis.

[5] In principle, we can validate propagation effects using small earthquakes, for which source effects are easily modeled, and for which nonlinearity is not a factor. In practice, the uneven distribution of earthquakes in the appropriate locations prevents this approach. For example, there are no recent, moderate-sized earthquakes along the San Andreas Fault in southern California that can be used to validate wave propagation effects from a scenario earthquake on that fault. Using the ambient seismic field, however, we can control the disposition of virtual seismic sources, and hence measure the response in areas of concern. In the following we show how the ambient field can be used to predict ground motion directly.

2. Methodology

[6] The idea that the point source response would emerge from cross correlation of the diffuse, ambient-noise seismic wavefields recorded by two different seismic stations has been around for decades [*Claerbout*, 1968]. This approach has been used successfully for helioseismology [*Rickett and Claerbout*, 1999], and more recently for the Earth itself, with significant advances in techniques for using the ambient field to retrieve the response of the Earth to a unit point force, i.e., the Green's function. Applications include surface-wave tomography [*Shapiro et al.*, 2005; *Sabra et al.*, 2005], volcano monitoring [*Sabra et al.*, 2006; *Brenguier et al.*, 2007], and petroleum prospecting [*Curtis et al.*, 2006]. Nearly all of these ambient noise studies focus on seismic wave arrival times, and in doing so apply sign-bit or other normalization to the data [*Campillo and Paul*, 2003; *Bensen et al.*, 2007]. This approach renders the data insensitive to non-stationary noise, but sacrifices information on the Green's function amplitude in the process [*Larose et al.*, 2007].

[7] Several studies have shown that it is possible to retrieve both travel times and amplitudes in the analysis of structural response [*Snieder and Safak*, 2006; *Kohler et al.*, 2007]. The amplitude decay with distance of the Green's function has also been experimentally obtained from noise correlations [*Larose et al.*, 2007]. In this study we use the ambient field to document basin amplification using the unit impulse response [*Bendat and Piersol*, 1993] for a station, near the San Andreas Fault, that can be thought of as a virtual

¹Department of Geophysics, Stanford University, Stanford, California, USA.

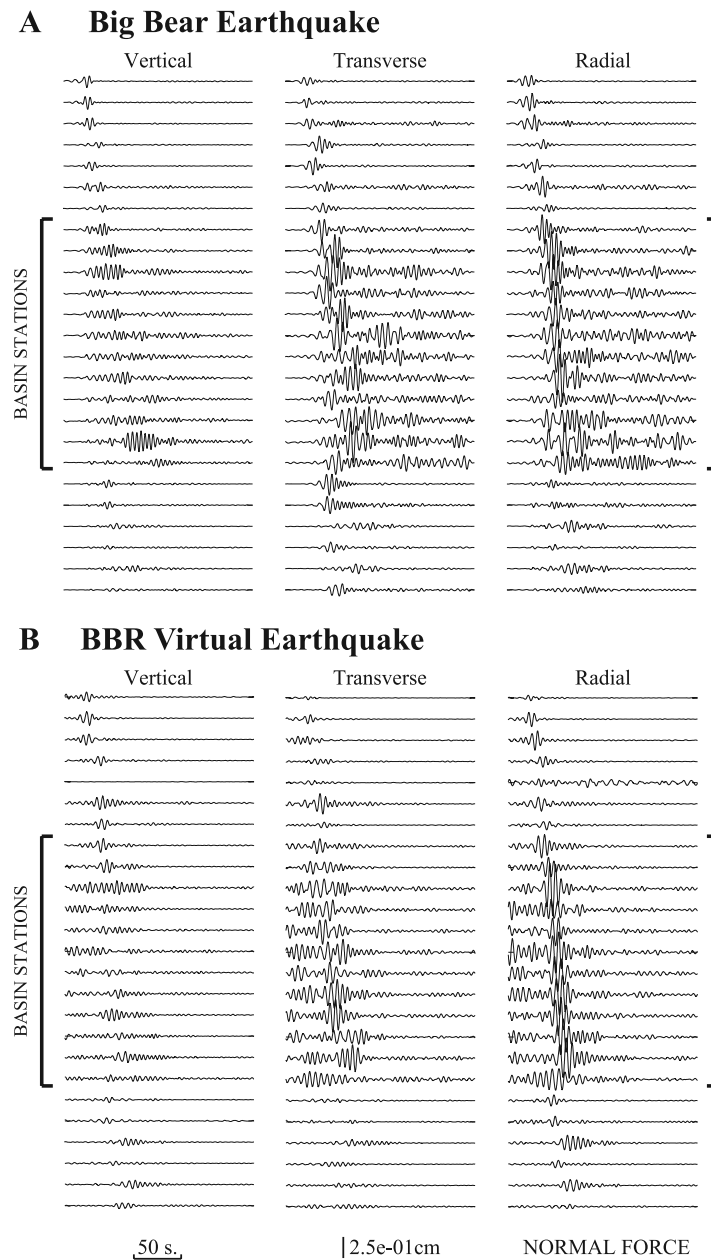


Figure 2. Amplification effects from the impulse response estimates and records from earthquake in Figure 1, band-pass filtered between 4 and 10 seconds. (a) Earthquake record section of rotated ground displacements for sites around the Los Angeles Basin. Records are plotted roughly with increased epicentral distance. The large brackets indicate sites within the basin. (b) Same as Figure 2a but for impulse response records for a horizontal force for reference station BBR. Note the amplification in the Los Angeles basin for both the impulse response as well as the earthquake records.

proportional to the square root of the propagation distance, consistent with the simplest possible surface wave propagation, is applied to isolate the basin amplification effects of interest, from geometrical spreading.

[13] The observed amplification is a function of the geological structure near the seismic stations, but it also depends on the direction of the incident seismic waves. This is evident from Figure 4, where we compare different virtual sources. The overall pattern for SVD and ADO is similar, showing strong basin amplification, but there are important differences, illustrating that the amplitudes depend on the location of the source. In the 4–10 second period range

used in this example, amplification is seen across the middle of the Los Angeles basin. This is consistent with the simulations of Southern San Andreas Fault earthquakes [Olsen *et al.*, 2006] that model wave propagation through a complex seismic velocity model for the area [Magistrale *et al.*, 2000; Kohler *et al.*, 2003].

4. Discussion and Conclusion

[14] Ambient-noise Green’s functions can be used to increase our knowledge of the velocity structure of three-dimensional crustal structure, which is important for accu-

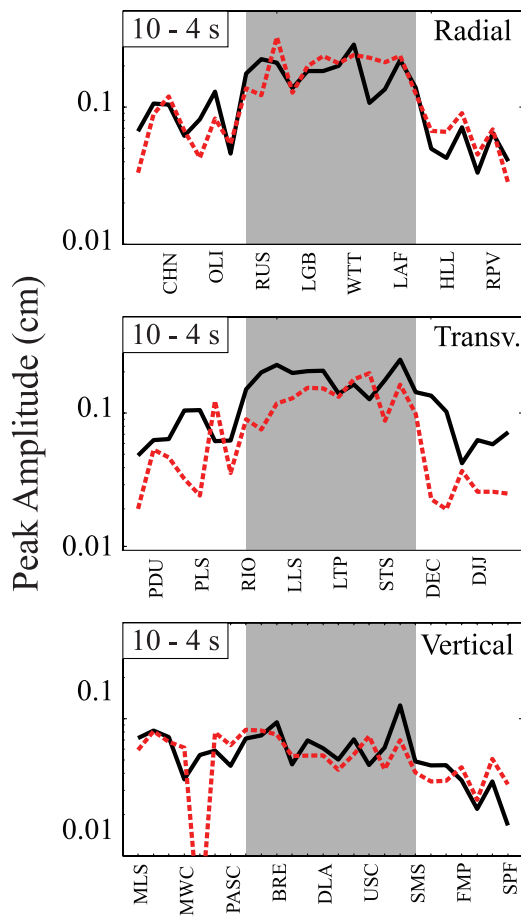


Figure 3. Peak amplitudes of earthquake (black) and impulse response records (red) for three-component ground displacement. Sites are plotted roughly with increasing epicentral distance and sites within the basin are indicated by gray shading. All stations from Figure 2 are used, for clarity only a few are marked in each plot. The horizontal components have significantly larger amplitudes with respect to the vertical component and show amplification effects at sites within the basin. The decreasing amplitude with distance for the vertical components is likely associated with geometrical spreading.

rate simulations of strong ground motion. The ambient-noise approach has the distinct advantage that it is “active,” in that seismologists can design experiments to determine station-to-station Green’s functions for ground motion estimates to target areas of particular concern. In addition these Green’s functions provide an important test and calibration for 3D velocity models used in numerical simulations (S. Ma et al., Testing community velocity models for southern California using the ambient seismic field, submitted to *Bulletin of the Seismological Society of America*, 2008).

[15] We have also shown that, at least in the period range of 4–10 seconds, it is possible to use ambient-noise Green’s functions directly, without the need for an intermediate step of estimating crustal velocity structure. These periods are outside the range of primary engineering interest (0.1 to 1 seconds), but they are quite relevant for the important case of long-period structures, such as bridges and very tall buildings [Heaton et al., 1995]. Extending the method to

shorter periods is an important research direction. Nevertheless, our results indicate the viability of an important new capability: direct ground motion prediction using the ambient field. It is not difficult to imagine an experiment that deploys broadband seismic instrumentation along the length of the southern San Andreas Fault, and stations in areas of interest in Los Angeles, to determine Green’s functions for modeling scenario earthquakes on the San Andreas Fault.

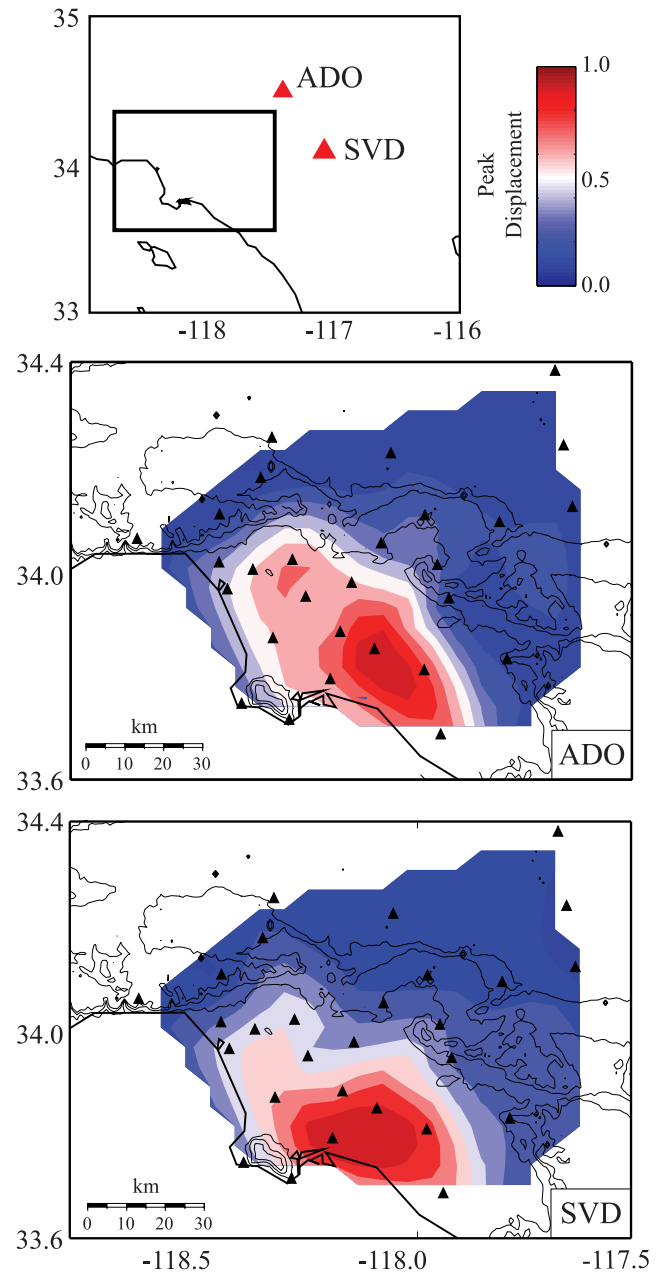


Figure 4. Amplification effects in the Los Angeles Basin between 4 and 10 seconds for different vertical virtual sources. Regional map shows seismic stations (ADO, SVD) and region of interest (box). Contour maps of normalized peak displacement amplitude from the impulse response for the two virtual sources are shown below. Basin amplification effects are slightly different for stations ADO and SVD due to differences encountered for different incident wave directions.

[16] **Acknowledgments.** We thank S. Ma, R. Snieder, F. Sanchez-Sesma, P. Gerstoft, and G. Papanicolaou for helpful discussions. SCEC contribution 1141.

References

- Aagaard, B. T., et al. (2008), Ground-motion modeling of the 1906 San Francisco earthquake, Part II: Ground-motion estimates for the 1906 earthquake and scenario events, *Bull. Seismol. Soc. Am.*, *98*, 1012–1046.
- Abrahamson, N., and K. Shedlock (1997), Overview, *Seismol. Res. Lett.*, *68*, 9–23.
- Bendat, J. S., and A. G. Piersol (1993), *Engineering Applications of Correlations and Spectral Analysis*, John Wiley Hoboken, N.J.
- Bensen, G. D., M. H. Ritzwoller, M. P. Barmin, A. L. Levshin, F. Lin, M. P. Moschetti, N. M. Shapiro, and Y. Yang (2007), Processing seismic ambient noise data to obtain reliable broad-band surface wave dispersion measurements, *Geophys. J. Int.*, *169*, 1239–1260, doi:10.1111/j.1365-246X.2007.03374.x.
- Brenguier, F., N. M. Shapiro, M. Campillo, A. Nercessian, and V. Ferrazzini (2007), 3-D surface wave tomography of the Piton de la Fournaise volcano using seismic noise correlations, *Geophys. Res. Lett.*, *34*, L02305, doi:10.1029/2006GL028586.
- Campillo, M., and A. Paul (2003), Long range correlations in the seismic coda, *Science*, *299*, 547–549.
- Claerbout, J. F. (1968), Synthesis of a layered medium from its acoustic transmission response, *Geophysics*, *33*, 264–269.
- Curtis, A., P. Gerstoft, H. Sato, R. Snieder, and K. Wapenaar (2006), Seismic interferometry—Turning noise into signal, *Leading Edge*, *25*, 1082–1092.
- Graves, R. W. (2008), The seismic response of the San Bernardino Basin region during the 2001 Big Bear Lake earthquake, *Bull. Seismol. Soc. Am.*, *98*, 241–252, doi:10.1785/0120070013.
- Heaton, T. H., J. H. Hall, D. J. Wald, and M. W. Halling (1995), Response of high-rise and base-isolated buildings to a hypothetical Mw 7.0 blind thrust earthquake, *Science*, *267*, 206–212.
- Kohler, M., H. Magistrale, and R. Clayton (2003), Mantle heterogeneities and the SCEC reference three-dimensional seismic velocity model version 3, *Bull. Seismol. Soc. Am.*, *93*, 757–774.
- Kohler, M. D., T. H. Heaton, and S. C. Bradford (2007), Propagating waves in the steel, moment-frame factor building recorded during earthquakes, *Bull. Seismol. Soc. Am.*, *97*, 1334–1345.
- Komatitsch, D., Q. Liu, J. Tromp, P. Süß, C. Stidham, and J. H. Shaw (2004), Simulations of ground motion in the Los Angeles Basin based upon the spectral-element method, *Bull. Seismol. Soc. Am.*, *94*, 187–206.
- Larose, E., P. Roux, and M. Campillo (2007), Reconstruction of Rayleigh-Lamb dispersion spectrum based on noise obtained from an air-jet forcing, *J. Acoust. Soc. Am.*, *122*(6), 3437–3444.
- Magistrale, H., S. M. Day, R. W. Clayton, and R. W. Graves (2000), The SCEC southern California reference three-dimensional seismic velocity model version 2, *Bull. Seismol. Soc. Am.*, *90*, S65–S76.
- Mai, P. M., and G. C. Beroza (2002), A spatial random field model to characterize complexity in earthquake slip, *J. Geophys. Res.*, *107*(B11), 2308, doi:10.1029/2001JB000588.
- Maruyama, T. (1963), On the force equivalents of dynamic elastic dislocations with reference to the earthquake mechanism, *Bull. Earthquake Res. Inst. Univ. Tokyo*, *41*, 467–487.
- Olsen, K. B., S. M. Day, J. B. Minster, Y. Cui, A. Chourasia, M. Faerman, R. Moore, P. Macchling, and T. Jordan (2006), Strong shaking in Los Angeles expected from southern San Andreas earthquake, *Geophys. Res. Lett.*, *33*, L07305, doi:10.1029/2005GL025472.
- Park, J., and V. Levin (2000), Receiver functions from multiple-taper spectral correlation estimates, *Bull. Seismol. Soc. Am.*, *90*, 1507–1520.
- Pitarka, A., K. Irikura, T. Iwata, and H. Sekiguchi (1998), Three-dimensional simulation of the near-fault ground motion for the 1995 Hyogo-Ken Nanbu (Kobe), Japan, earthquake, *Bull. Seismol. Soc. Am.*, *88*, 428–440.
- Power, M., B. Chiou, N. Abrahamson, Y. Bozorgnia, T. Shantz, and C. Roblee (2008), An overview of the NGA project, *Earthquake Spectra*, in press.
- Rickett, J., and J. F. Claerbout (1999), Acoustic daylight imaging via spectral factorization: Helioseismology and reservoir monitoring, *Leading Edge*, *18*, 957–960.
- Sabra, K. G., P. Gerstoft, P. Roux, W. A. Kuperman, and M. C. Fehler (2005), Extracting time-domain Green's function estimates from ambient seismic noise, *Geophys. Res. Lett.*, *32*, L03310, doi:10.1029/2004GL021862.
- Sabra, K. G., P. Roux, P. Gerstoft, W. A. Kuperman, and M. C. Fehler (2006), Extracting coherent coda arrivals from cross-correlations of long period seismic waves during the Mount St. Helens 2004 eruption, *Geophys. Res. Lett.*, *33*, L06313, doi:10.1029/2005GL025563.
- Seed, H. B., and I. M. Idriss (1971), Simplified procedure for evaluating soil liquefaction potential, *J. Soil Mech. Found. Div. Am. Soc. Civ. Eng.*, *97*, 1249–1273.
- Shapiro, N. M., M. Campillo, L. Stehly, and M. H. Ritzwoller (2005), High-resolution surface-wave tomography from ambient seismic noise, *Science*, *307*, 1615–1618.
- Snieder, R., and E. Safak (2006), Extracting the building response using seismic interferometry: Theory and application to the Millikan Library in Pasadena, California, *Bull. Seismol. Soc. Am.*, *96*, 586–598.
- Stehly, L., M. Campillo, and N. Shapiro (2006), A study of the seismic noise from its long-range correlation properties, *J. Geophys. Res.*, *111*, B10306, doi:10.1029/2005JB004237.
- Stidham, C., M. Antolik, D. Dreger, S. Larsen, and B. Romanowicz (1999), Three-dimensional structure influences on the strong-motion wavefield of the 1989 Loma Prieta earthquake, *Bull. Seismol. Soc. Am.*, *89*, 1184–1202.
- Vidale, J. E., and D. V. Helmberger (1988), Elastic finite-difference modeling of the 1971 San Fernando, California earthquake, *Bull. Seismol. Soc. Am.*, *78*, 122–141.

G. C. Beroza and G. A. Prieto, Department of Geophysics, Stanford University, 397 Panama Mall, Stanford, CA 94305-2215, USA. (beroz@pangea.stanford.edu; gprieto@stanford.edu)